Since January 2020 Elsevier has created a COVID-19 resource centre with free information in English and Mandarin on the novel coronavirus COVID-19. The COVID-19 resource centre is hosted on Elsevier Connect, the company's public news and information website.

Virus Research 286 (2020) 198088

Contents lists available at ScienceDirect

Virus Research

journal homepage: www.elsevier.com/locate/virusres

Pyruvate affects inflammatory responses of macrophages during influenza A virus infection

Hazar Abusalamah[1], Jessica M. Reel[1], Christopher R. Lupfer*

Department of Biology, Missouri State University, 901 S. National Ave. Springfield, MO, 65897, USA

ARTICLE INFO

Keywords:
Inflammation
Influenza A virus
Pyruvate
Antioxidant
Inflammasome

ABSTRACT

Pyruvate is the end product of glycolysis and transported into the mitochondria for use in the tricarboxylic acid (TCA) cycle. It is also a common additive in cell culture media. We discovered that inclusion of sodium pyruvate in culture media during infection of mouse bone marrow derived macrophages with influenza A virus impaired cytokine production (IL-6, IL-1β, and TNF-α). Sodium pyruvate did not inhibit viral RNA replication. Instead, the addition of sodium pyruvate alters cellular metabolism and diminished mitochondrial reactive oxygen species (ROS) production and lowered immune signaling. Overall, sodium pyruvate affects the immune response produced by macrophages but does not inhibit virus replication.

1. Introduction

Pyruvate (Pyr) ($C_3H_4O_3$) is a central molecule in cellular metabolism. In addition to the typical glycolysis-to-TCA pathway (Barnett, 2003), Pyr can be derived from lactate taken up from outside the cells or synthesized intracellularly from amino acids (Halestrap and Price., 1999; Karmen et al., 1955). Instead of entering the TCA cycle, anaerobic glycolysis can occur (fermentation) where Pyr is reduced into lactate in order to regenerate NAD^+. In rapidly dividing cells, like some immune cells or cancer cells, this also occurs even when oxygen is present (aerobic glycolysis/Warburg effect) (Roiniotis et al., 2009). Although energetically less favorable, aerobic glycolysis facilitates metabolite production necessary for rapid cell division, such as amino acid and nucleic acid synthesis (Vander Heiden et al., 2009). Reports have shown that IAV infection severely alters metabolism including amino acid and lipid metabolism (Chandler et al., 2016).

The innate immune system has germline-encoded pattern-recognition receptors (PRRs). These sensors are capable of recognizing microorganisms that invade the host (Akira et al., 2006). PRRs can bind to pathogen-associated molecular patterns (PAMPs) such as RNA from viral genomes (Crozat and Beutler., 2004). Detection of PAMPs by PRRs activates a variety of immune signaling pathways resulting in cytokines production, increased phagocytosis and cell death. However, these responses can be modulated by metabolic processes. When retinoic acid inducible gene-I (RIG-I) is activated by cytoplasmic viral RNA, it moves to the mitochondria, where it interacts with Mitochondrial Antiviral Signaling protein (MAVS) (Kato et al., 2006). MAVS then recruits adaptors proteins at the mitochondria forming the MAVS signalosome, which activates the transcription factors IRF3/7 and NF-κB (Seth et al., 2005). However, lactate can inhibit this pathway, thus dampening inflammation during viral infection (Zhang et al., 2019).

The inflammasome is another immune signaling pathway that forms a multiprotein complex, which activates the cysteine protease caspase-1 (Agostini et al., 2004). Active caspase-1 then activates the inflammatory cytokines interleukin (IL)-1β and IL-18 (Sutterwala et al., 2006). Inflammasome activation by NOD-like receptor containing a pyrin 3 (NLRP3) is somewhat unique, as its main activation signals are cellular damage including oxidative stress and potassium efflux (Allen et al., 2009; Petrilli et al., 2007). Intriguingly, NLRP3 appears to be tuned-in to the metabolic state of cells through glycolysis (Moon et al., 2015; Xie et al., 2016).

Pyr is well studied in metabolism, but its role in the immune response is not. During the course of infecting macrophages with IAV, we noted that different brands of cell culture media with different nutrient compositions affected the magnitude of the immune response. In particular, the inclusion of sodium pyruvate (NaPyr) in culture media inhibited immune signaling during IAV infection. Here we show that NaPyr added to BMDM cell culture media inhibits the release of important pro-inflammatory cytokines IL-1β, IL-6, and TNF-α. In addition to these findings, we observed that addition of NaPyr does not inhibit viral replication, rather it suppresses the immune response to IAV through altering metabolism and ROS production.

* Corresponding author.
E-mail address: ChristopherLupfer@missouristate.edua (C.R. Lupfer).
[1] These authors contributed equally to this manuscript.

https://doi.org/10.1016/j.virusres.2020.198088
Received 4 February 2020; Received in revised form 26 June 2020; Accepted 1 July 2020
Available online 04 July 2020

2. Materials and methods

2.1. Animal welfare

WT C57BL/6 J mice were bred and raised in the Temple Hall Vivarium at Missouri State University. Mice were euthanized via CO_2 asphyxiation and cervical dislocation and bone marrow collected for differentiation into macrophages. All breeding and experiments were performed in accordance with Institutional Animal Care and Use Committee (IACUC) guidelines (protocols 16.009 and 19.019), the AVMA Guidelines on Euthanasia, NIH regulations (Guide for the Care and Use of Laboratory Animals), and the U.S. Animal Welfare Act of 1966.

2.2. Generation of bone marrow macrophages

Bone Marrow Derived Macrophages (BMDM) were produced by harvesting bone marrow from the femur and tibia of 7−14-week-old C57BL/6 J mice. Bone marrow cells were then grown for 5 days in bone marrow differentiation media, which consisted of Dulbecco's Modified Eagle Medium (DMEM) + 10 % FBS + 1% Pen/Strep + 1% Non-essential amino acids (NEAA) and supplemented with L929 cell conditioned media. L929 cell conditioned medium contains Macrophage colony-stimulating factor (M-CSF) and was produced by growing L929 cells in DMEM + 10 % FBS + 1% Pen/Strep for 10 days and then filtering the media via a 0.2 μm filter.

On day 5 of BMDM growth, cells were scraped and re-plated into 12-well plates at 1×10^6 cells/well in 1 mL BMDM media and incubated overnight to allow cells time to adhere to the plates. Macrophages were used the following day for experiments.

2.3. Virus production

The strain of IAV used in all experiments is influenza A/PR/8/34 H1N1. In order to generate virus, we inoculated pathogen-free hen's eggs with 1000 PFU of IAV. 3 days post inoculation, the allantoic fluid was harvested, centrifuged to remove debris, and frozen at −80 °C for later use.

2.4. Viral plaque assay

The IAV plaque assay was performed using MDCK cells seeded at 3×10^5 cells/well in 12-well plates in DMEM + 5% FBS + 1%Pen/Strep. 10-fold dilutions of the virus were prepared in MEM without FBS. MDCK cells were washed with PBS twice and 100 μL of each virus dilution were added to duplicate wells in 12-well plates and incubated at 37 °C and 5% CO_2 for one hour. Semisolid overlay was prepared as previously described (Lupfer et al., 2008). TPCK-trypsin was added to a final concentration of 1.0 μg/mL. After the full hour of incubation, infection medium was removed from 12-well plates, and 2 mL of the warm overlay with TPCK trypsin was added to each well and allowed to solidify. Plates were turned upside down and incubated for 3 days. After 3 days, the overlaid agar was removed and plaques counted after staining with 1% crystal violet in methanol.

2.5. Enzyme-Linked immunosorbent assay (ELISA)

Cell culture supernatants collected from infected and control BMDM were analyzed for IL-1β, TNF- α, and IL-6. ELISA kits were purchased from Ebioscience (88−7013-88, 88−7324-88, 88−7064-88) and assays performed according to the manufacturer's recommendations. Plates were read at 450 nm on a microplate reader (BioTek ELx808).

2.6. Western blotting

Cell lysates were collected by adding RIPA buffer with protease and phosphatase inhibitors (Thermo Scientific, PIA32959, PIA32957) to BMDM treated or infected as indicated. 4x SDS loading dye was then added to samples, which were boiled for 20 min and resolved by SDS-PAGE and then transferred to PVDF membranes. Western blotting for caspase-1 (caspase-1 p45 and p20), phosphorylated IκBα and total IκBα were then performed by incubating membranes in primary antibody diluted in 5% milk in TBST overnight at 4 °C (See Table 1 for a list of antibodies). The next day, membranes were washed 3x in TBST buffer and incubated for 45 min in secondary antibody diluted in 5% milk in TBST (Table 1). Membranes were washed again, and images obtained using Super Signal West Fempto substrate (ThermoFisher, A53225) and an Azure C300 digital imaging system.

Table 1
Antibodies.

Antibodies	Catalog Number
Rabbit anti-mouse β-Actin	Cell Signaling Technology, 8457S
Rabbit anti-mouse IκB-α	Cell Signaling Technology, 9242S
Rabbit anti-mouse Phospho-IκB-α	Cell Signaling Technology, 2859S
Mouse anti-mouse Caspase-1	Adipogen, 661,228
Anti-Rabbit-HRP secondary	Jackson Immuno Res.111−035-144
Anti-mouse-HRP secondary	BioRad, HAF007

2.7. Cell death and ROS

Macrophages were plated in 12-well plates and infected and/or treated as indicated. After 24 h, and 30 min before collecting samples, cells were stained with a mitochondrial specific ROS sensitive dye (2.5 nM Mitosox; ThermoFisher, M36008) or a cell death stain (5 mM SYTOX-red; ThermoFisher, S34859). After 30 min, the media was removed and 1 mL of PBS was added to each well and the macrophages were scraped off the wells. Cells were analyzed on an ACURI C6 or Attune NxT flow cytometer. 10,000 cells per sample were analyzed for fluorescence intensity and percentage of cells positive for each dye.

2.8. Analysis of Gene expression

BMDM were infected and treated as indicated and samples were collected at 6, 12, and 24 h after infection. Media was removed and 500 μL Trizol (Invitrogen, AM9738) was added to samples and incubated for 5 min at room temperature. RNA was then isolated according to the manufactures protocol. All samples were normalized to 200 ng/μl RNA in nuclease-free water. The High Capacity cDNA Reverse Transcriptase kit (Thermo Fisher Scientific 436,881) was then used to convert 1ug RNA into cDNA. Then, cDNA was diluted 1:5 in nuclease-free water, and 5 μL cDNA was used per reaction to perform qRT-PCR with the DyNAmo HS SYBR Green qPCR master mix (Thermo Scientific 00,596,849) according to the manufacturer's instructions using a STRATAGENE-Mx3005 P PCR machine. (See Table 2 for Primer Sequences).

2.9. Examination of cellular ATP

BMDM were infected and treated as indicated, with IAV infected samples collected at 12 and 24 h post infection. LPS + ATP samples were collected at 4 h post LPS treatment with ATP added for the final 30 min. Samples were analyzed using a StayBrite Highly Stable ATP Bioluminescence Assay kit (BioVision, K791−100) according to the kit instructions. To collect cell samples, the culture supernatant was removed, cells were washed 3x with 5 mL DPBS, and then, 100 μL of 1X RIPA buffer was added to each well. Cells lysate was collected and centrifuged at 12,000xg for 30 s. 10 μL of each cell lysate was pipetted into enzyme/buffer mix, and then analyzed quickly using the GloMax Jr. by ProMega on the GloBrite module, in RLUs.

Table 2
Primer Sequences.

Primers	Sequence 5′–3′
β-Actin forward	GGCTGTATTCCCCTCCATCG
β-Actin reverse	CCAGTTGGTAACAATGCCATGT
IL-1β forward	GACCTTCCAGGATGAGGACA
IL-1β reverse	AGCTCATATGGGTCCGACAG
TNF-α forward	CATCTTCTCAAAATTCGAGTGACAA
TNF-α reverse	TGGGAGTAGACAAGGTACAACCC
IL-6 forward	TCCAGTTGCCTTCTTGGGAC
IL-6 reverse	GTACTCCAGAAGACCAGAGG
IFN-β forward	GCCTTTGCCATCCAAGAGATGC
IFN-β reverse	ACACTGTCTGCTGGTGGAGTTC
IAV M1 forward	TGAGTCTTCTAACCGAGGTC
IAV M1 reverse	GGTCTTGTCTTTAGCCATTCC
IAV NP forward	CTCGTCGCTTATGACAAAGAAG
IAV NP reverse	AGATCATCATGTGAGTCAGAC

2.10. Lactate production assay

BMDM were infected and treated as indicated and the supernatant collected at 24 h post infection. The supernatant was then centrifuged at 14,000xg for 1 min to remove cell debris. Samples were analyzed using the Eton Bioscience L-Lactate Assay kit I (SKU# 1,200,011,002) according to kit directions. Plates were read at 490 nm on a microplate reader (BioTek ELx808).

2.11. In vitro pyruvate treatment

1×10^6 macrophages were plated in 12-well plates overnight. The next day, cells were washed 2x with PBS. Then, 200 μL of RPMI 1640 without serum or NaPyr and with L-glutamine was added to BMDM. 2.5×10^7 PFU of IAV (25MOI) was added to some wells and other wells were left uninfected as controls. Uninfected controls and IAV infected BMDM were also either untreated or treated with 1 mM NaPyr (HyClone, SH30239.01). Plates were incubated at 37 °C and 5% CO_2 for two hours with shaking. Then, 200 μL RPMI + 20 % FBS was added to each well. Additional NaPyr was added to appropriate wells to maintain the 1 mM concentration. Samples were collected at 6, 12, and 24 h after IAV infection. The delayed addition of FBS is required for IAV infection of BMDM.

To test the effects of NaPyr on the immune response of BMDM to other stimuli, 1×10^6 BMDM were plated per well in 12-well plates. The next day, BMDM were washed 2x with PBS and 400 μL of RPMI 1640 + 10 % FBS and L-glutamine but without NaPyr was added to each well. Some wells were treated with 1 μg/mL LPS for 4 h with inclusion of 5 mM ATP (Sigma, L3129 and Acros, 102,800,100) for the last 30 min. Some wells were also treated with 1, 2 or 5 mM NaPyr. Samples were collected at the end of 4 h of treatment. Poly I:C samples were treated with 25 μg/mL as indicated above and supernatants collected 24 h post treatment.

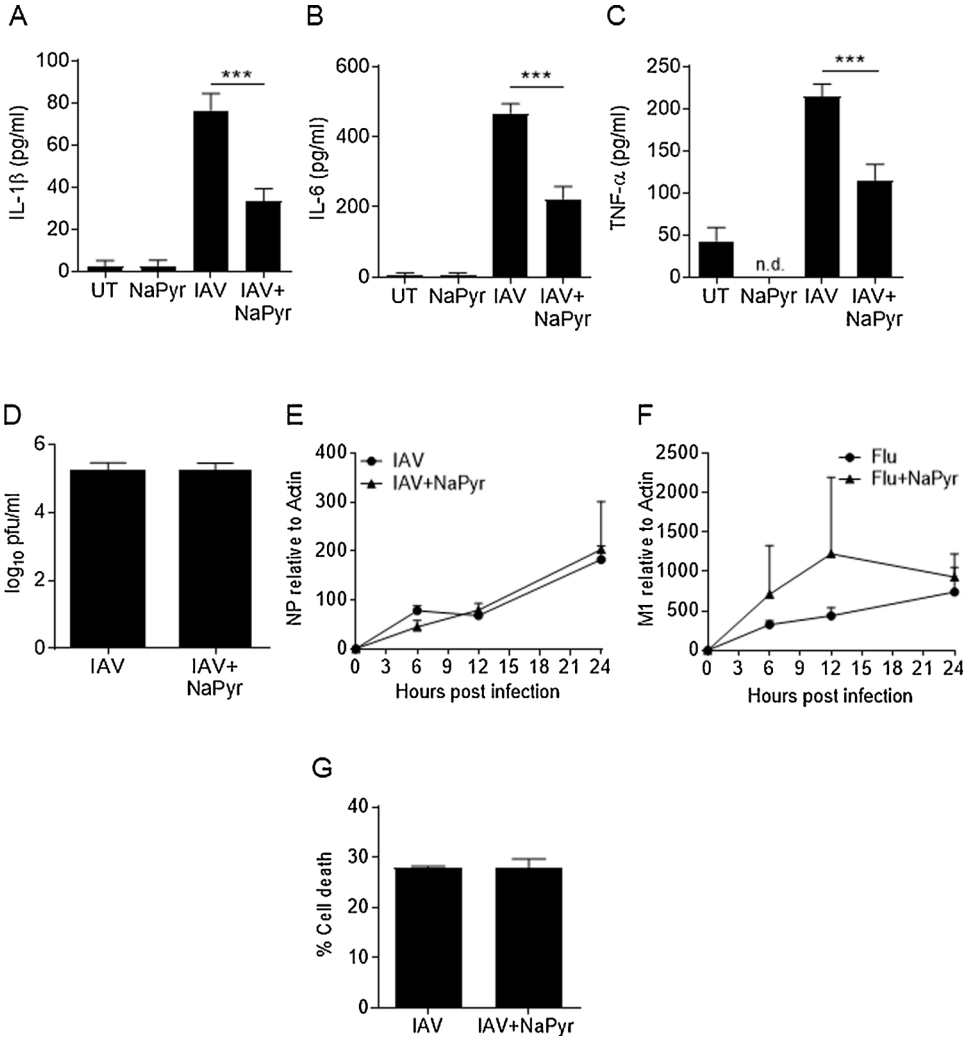

Fig. 1. Pyruvate inhibits cytokine responses but not virus replication.
BMDM were mock infected (untreated = UT) or infected with 10MOI influenza A/PR8/34/H1N1 virus (IAV) in the presence or absence of sodium pyruvate (NaPyr). After 24 h, cell culture supernatants were collected and examined for cytokine expression by ELISA (A–C) or examined for virus titer by plaque assay (D). Total RNA was isolated from BMDM at the indicted time points after IAV infection in the presence or absence of NaPyr. RNA was transcribed into cDNA and qRT-PCR performed for the indicated viral genes (E–F). BMDM were infected for 24 h in the presence or absence of NaPyr and stained with Sytox-Red then examined by flow cytometry for percentage of cell death (G). Data are representative of 2–4 independent experiments with n = 2–3 wells per experiment. Statistical significance was determined using the students T-test for single comparisons, one-way ANOVA with Tukey post-hoc for multiple comparisons. *** $p < 0.001$

2.12. Statistical analysis

Statistical analysis was performed using GraphPad PRISM6. Comparison of 2 conditions was performed using the 2-sided student's *t*-test. Comparison of multiple conditions was performed using the One-Way ANOVA with Tukey's post-hoc test. A p-value < 0.05 was considered statistically significant.

3. Results

3.1. NaPyr affects the immune response, not virus replication

In discussion with other researchers (personal communication, Teneema Kurikose, St Jude Children's Research Hospital), we discovered the use of media from different suppliers impacted the magnitude of the immune response by bone marrow derived macrophages (BMDM) during IAV infection. Specifically, BMDM infected with IAV in Dubelco's Modified Eagle's Medium (DMEM) purchased from Sigma Aldrich (Catalogue # D5671) produced elevated cytokine responses compared to IAV infected BMDM cultured in DMEM purchased from ThermoFisher Scientific (Corning MT10013CV or Gibco11995040). We also noted that bone marrow derived dendritic cells (BMDC) generally produce higher cytokine levels than BMDM in response to IAV infection, but BMDC are typically cultured in RPMI 1640. We examined the composition of these media and determined that NaPyr was associated with lower immune responses. Therefore, we infected BMDM with IAV in RPMI1640 medium with and without NaPyr. Our data demonstrate that addition of NaPyr significantly impaired cytokine production by BMDM infected with IAV (Fig. 1A–C).

We next examined virus replication by collecting cell culture media from infected BMDMs 24 h after infection and performing viral plaque assays. BMDM are refractory to infection with some strains of IAV (Cline et al., 2017), but similar levels of functional virions were recovered from BMDMs in our model with or without NaPyr treatment (Fig. 1D). As virion production was low overall, we further confirmed that NaPyr did not affect virus growth or its ability to infect macrophages by examining viral RNA levels (IAV M1 and NP genes). NaPyr did not inhibit the replication of virus RNA, demonstrating that NaPyr does not affect cytokine responses by inhibiting IAV replication (Fig. 1E–F). In addition, NaPyr treatment of IAV infected BMDM had no effect on cell death (Fig. 1G).

3.2. NaPyr inhibits immune signaling pathways

We examined cytokine gene expression by RT-PCR at 6, 12, and 24 h after IAV infection. NaPyr did have an inhibitory effect on gene expression in IAV infected BMDM compared to virus infected BMDM cultured in the absence of NaPyr (Fig. 2A–D). We performed western blotting on cell lysates from BMDM infected with IAV and treated with NaPyr but did not observe any significant differences in the activation of NF-κB (phospho-IκBα) (Fig. 2E–F). However, NaPyr inhibited caspase-1 activation in BMDM infected with IAV (Fig. 2G–H).

To determine if NaPyr treatment broadly inhibited immune signaling, we treated BMDM with lipopolysaccharide (LPS) and adenosine triphosphate (ATP), which is a potent activator of the NLRP3 inflammasome (Mariathasan et al., 2006). Intriguingly, LPS + ATP treated BMDM cultured with NaPyr produced similar amounts of IL-1β, IL-6, and TNF compared to control infected cells (Fig. 3A–C). Furthermore, caspase-1 activation was not inhibited, even at higher doses of NaPyr than used with IAV (Fig. 3D–E).

To determine if NaPyr's anti-inflammatory properties were linked to viral ligands as opposed to bacterial ligands, we stimulated BMDM with the TLR3 ligand poly I:C (PIC). Interestingly, BMDM treated with PIC and cultured with NaPyr produced similar amounts of IL-6 compared to the untreated controls (Fig. 3F).

3.3. Anti-inflammatory effects of NaPyr are associated with altered metabolism in BMDM

Previously, NaPyr was reported to be an antioxidant with potential therapeutic uses in a variety of inflammatory diseases (Ramos-Ibeas et al., 2017; Votto et al., 2008). NLRP3 activation in many instances is dependent on reactive oxygen species (ROS) and mitochondrial damage (Lupfer et al., 2013, 2014; Heid et al., 2013). NF-κB signaling can also be modulated by ROS (Morgan and Liu, 2011). Thus, we examined the antioxidant capacity of NaPyr in BMDM infected with IAV or LPS + ATP treated BMDM by staining with the mitochondrial ROS sensitive dye MitoSOX. IAV infection increased mitochondrial ROS generation and addition of NaPyr lowered mitochondrial ROS during IAV infection (Fig. 4A–B). During LPS + ATP treatment, mitochondrial ROS was elevated, but NaPyr had no effect on ROS in this setting (Fig. 4A, C). These results indicate that NaPyr inhibits ROS in a context specific manner.

IAV replication requires a massive metabolic burst to produce not only the viral nucleotides and proteins for virus replication, but also the antiviral immune responses of the cell. Previous research has shown that IAV induces a unique and elevated catabolic profile including increased lactate production (Smallwood et al., 2017). Elevated lactate levels have been reported to inhibit RIG-I signaling, which could explain our observations (Zhang et al., 2019). We examined lactate production from BMDM and observed a significant increase in lactate caused by IAV infection alone, but this was not enhanced by the addition of NaPyr (Fig. 4D). We thus hypothesized that NaPyr may fulfil a metabolic need during IAV infection, as opposed to the formation of a byproduct. We examined intracellular ATP production by BMDMs infected with IAV and found that IAV infection results in increased ATP levels over uninfected BMDM or LPS + ATP treated BMDM (Fig. 4E). Importantly, NaPyr treatment was able to transiently boost ATP output from BMDM to match the need seen in IAV infected cells (Fig. 4E). As the ATP needs of IAV infected cells were not copied by LPS + ATP, NaPyr may specifically decrease mitochondrial ROS during IAV infection by balancing metabolic stress.

4. Discussion

The ability of metabolites to affect the immune response to infection is an important area of research with implications for preventing and treating disease. Recent research shows that changes in metabolism in cells of the immune system can affect diseases such as influenza, cancer, diabetes and more (Matarese et al., 2008; Shi et al., 2011; Diers et al., 2012). Our data clearly indicate that treatment of IAV infected macrophages with NaPyr can reduce cytokines production (IL-1β, TNF-α, and IL-6). However, NaPyr does not affect virus titer or RNA replication in macrophages. Instead, NaPyr alters the immune function of the macrophages.

Antioxidants that can prevent mitochondrial damage also prevent NLRP3 inflammasome activation and release of IL-1β from infected cells (Lupfer et al., 2013, 2014). Previous reports indicate that NaPyr can decrease inflammation by its antioxidant potential (Ramos-Ibeas et al., 2017; Das, 2006; Xia et al., 2016). Although NaPyr may function as a ROS scavenger, we further propose that NaPyr reduces metabolic stress and ROS generation in an infection or disease specific manner. Specifically, pyruvate is taken into cells and bypasses many of the regulatory checkpoints for energy metabolism such as glucose transporters and phosphofructokinase (Schell and Rutter., 2013; Trompette et al., 2018). It can be directly transported into the mitochondria for use in the TCA cycle and ATP production or used in anabolic pathways (Brand and Nicholls., 2011). Thus, addition of NaPyr to cells increases ATP production, as we observed, and likely affects additional metabolic pathways. In our model, we propose that decreased mitochondrial ROS is thus a secondary, but important, anti-inflammatory effect of NaPyr treatment. There are also additional factors that may affect the ability

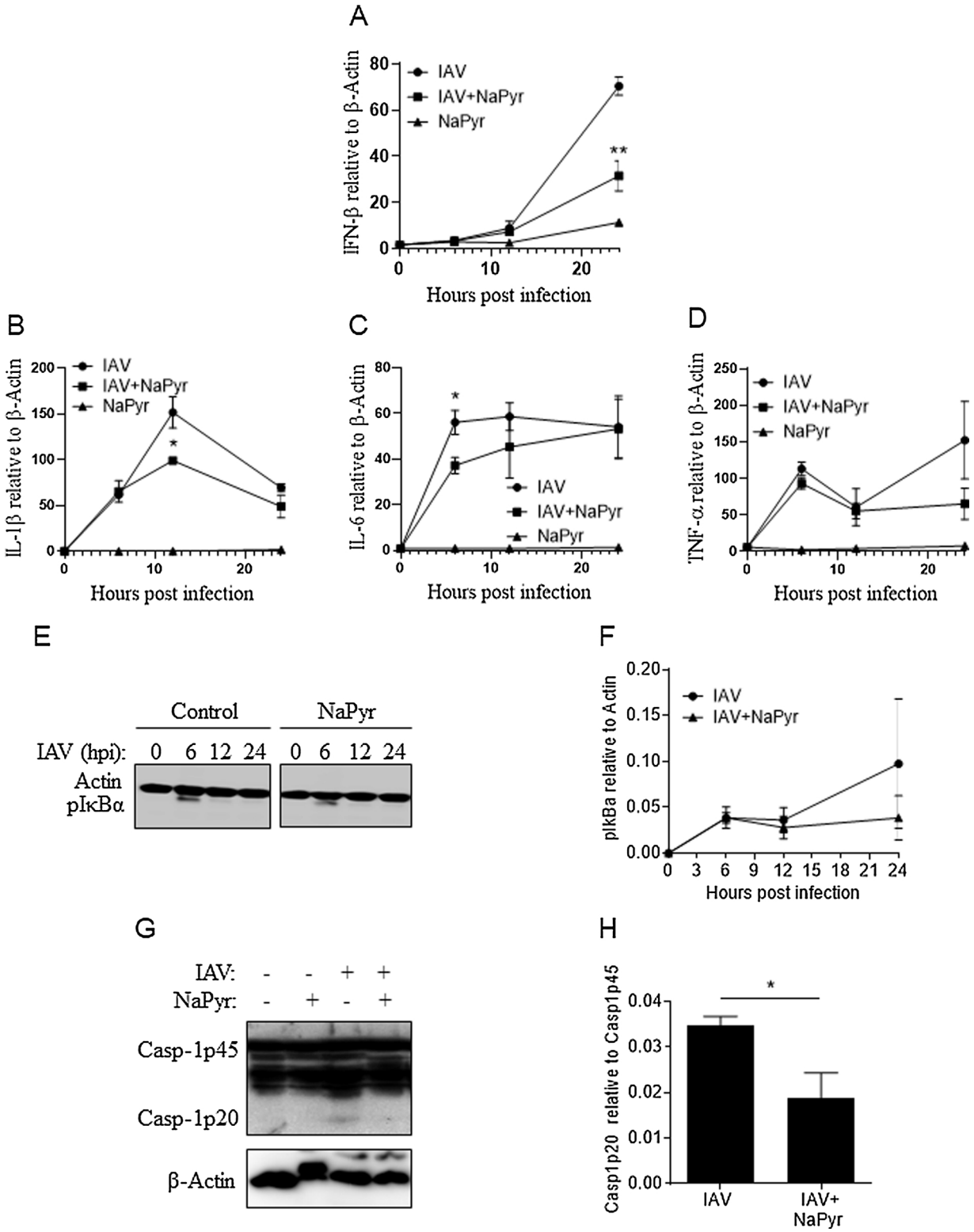

Fig. 2. Pyruvate inhibits immune signaling during IAV infection.
BMDM were mock infected (untreated = UT) or infected with 10MOI IAV with our without NaPyr. Total RNA was isolated from BMDM at the indicted time points after IAV infection in the presence or absence of NaPyr. RNA was transcribed into cDNA and qRT-PCR performed for the indicated cytokine genes (A–D). Cell lysates were collected at the indicated time points after IAV infection of BMDM in the presence or absence of NaPyr and examined by western blotting for NF-κB activation (phosphorylated-IκBα) (E–F) or caspase-1 activation (Casp-1p20) after 24 h (G–H). Data are representative of 2–4 independent experiments with n = 2–3 wells per experiment. Statistical significance was determined using the students T-test for single comparisons, one-way ANOVA with Tukey post-hoc for multiple comparisons. * $p < 0.05$, ** $p < 0.01$

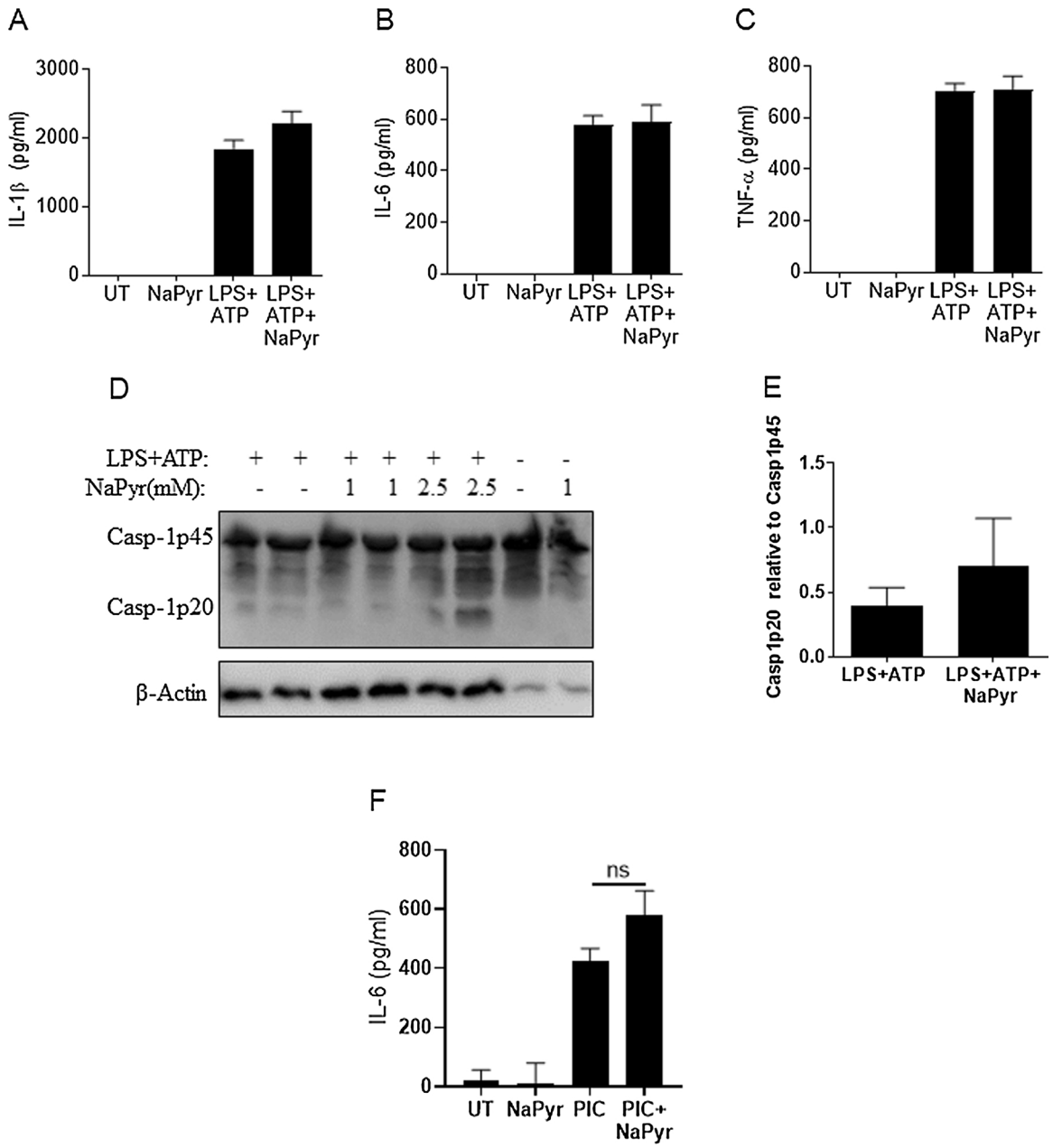

Fig. 3. Immune responses to LPS + ATP are not affected by NaPyr.
BMDM were mock treated (untreated = UT) or treated with 1μM LPS for 3.5 h and then treated with 5 mM ATP for 0.5 h in the presence or absence of NaPyr. Culture supernatants and cell lysates were collected after the total 4 h treatment and examined by ELISA for cytokine production (A–C) or by western blot for caspase-1 activation (Casp-1p20) (D–E). BMDM were mock treated (untreated = UT) or treated with 25μM poly I:C (PIC) in the presence or absence of NaPyr (F). Data are representative of 2–4 independent experiments with n = 2–3 wells per experiment. Statistical significance was determined using the students T-test test for single comparisons, one-way ANOVA with Tukey post-hoc for multiple comparisons. No results were significantly different.

of NaPyr to inhibit other stimuli. In the case of LPS + ATP treatment, the treatment duration is much shorter than IAV (only 4 h for LPS + ATP instead of 24 h for IAV). Thus, intrinsic differences in the timing and pathways of the different stimuli may further impact the effects of NaPyr and should be examined further.

In conclusion, NaPyr affects cytokine production by inhibiting inflammatory signaling pathways and not by affecting virus growth or cell death in macrophages. Metabolic pathways are important for cellular activation and have documented roles in immune signaling and immune cell function (Chandler et al., 2016; Roiniotis et al., 2009; Moon et al., 2015; Xie et al., 2016; Smallwood et al., 2017). Understanding the effects NaPyr has on the immune response to IAV and other infections will help elucidate the immune response in general and determine if certain nutrients can improve the immune response. Furthermore, severe IAV infection in human patients is associated with a metabolic crisis (especially depleted ATP) resulting in multi organ failure (Kido et al., 2016). As pyruvate clearly increases ATP production, decreases ROS and limits inflammation during IAV infection, it is worth examining as a potential therapeutic option in this and other diseases. Finally, severe infections with IAV and the current COVID19 pandemic are both associated with a “cytokine storm” that results in severe immunopathology (Han et al., 2020; Huo et al., 2018). Corticosteroids are used in severe cases to suppress this overt inflammation. Importantly, the only drug to date that has demonstrated clinical benefit for COVID19 is dexamethasone (Horby et al., 2020; Selvaraj et al., 2013). Unfortunately, corticosteroids may leave the host susceptible to

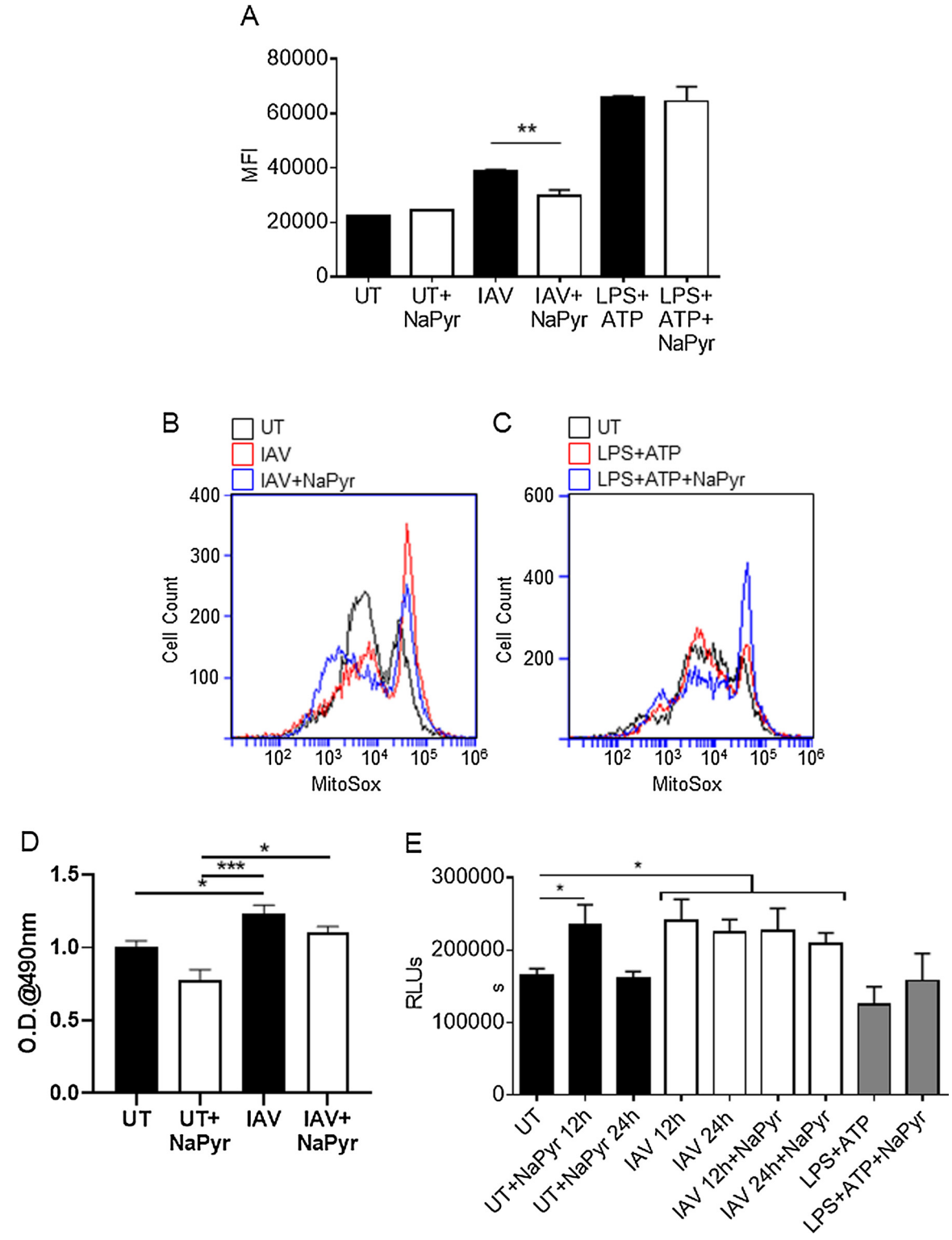

Fig. 4. Altered immune signaling is associated with ROS and ATP levels.
BMDM were mock infected (untreated = UT) or infected with 10MOI IAV for 24 h or treated with 1μM LPS for 3.5 h and then treated with 5 mM ATP for 0.5 h, in the presence or absence of NaPyr. Cells were then stained with MitoSox and mitochondrial ROS levels determined by flow cytometry (MFI = Median Fluorescence Intensity) (A–C). Cell supernatants were examined for lactate (D) and lysates were also examined for ATP levels (E). Data are representative of 3–4 independent experiments with n = 2–3 wells per experiment. Statistical significance was determined using the students T-test for single comparisons, one-way ANOVA with Tukey post-hoc for multiple comparisons. * $p < 0.05$, ** $p < 0.01$, *** $p < 0.001$

outgrowth of the initial pathogen or to secondary infection (Theoharides and Conti., 2020). As we observed no significant change in virus replication in this model, NaPyr may have therapeutic benefit for severe IAV and other infections where excessive inflammation is a key factor. N115 is an FDA approved NaPyr based nasal spray (Emphycorp, Inc) currently used for the treatment of patients with COPD and Idiopathic Pulmonary Fibrosis, that has been shown safe and effective in phase I/II/III clinical trials. Importantly, N115 significantly

decreased nasal and lung inflammation including IL-6 and improved measures of lung function including FEV-1, SaO2, FVC, FEV-1/FVC ratios (Votto et al., 2008, and personal communication with Dr. Alain Martin, Emphycorp, Inc.). Clinical trials using inhaled sodium pyruvate (N115) for COVID-19 infected patients are currently in progress to determine if the inhalation of sodium pyruvate can reduce the severity of lung inflammation in this disease.

Author statement

HA, JMR helped to conceptualize the project, collect and analyze the data and helped write the manuscript. CRL conceptualized the project, developed methodology, managed the project and resources, analyzed the data, wrote and approved all drafts of the manuscript.

Acknowledgements

We thank Teneema Kurikose, St Jude Children's Research Hospital, for helpful discussion in the initial stages of this research. We also thank Missouri State University for research funding through Faculty Startup funds to CRL and Graduate Student Research funds to HMA and JMR.

Appendix A. Supplementary data

Supplementary material related to this article can be found, in the online version, at doi:https://doi.org/10.1016/j.virusres.2020.198088.

References

Agostini, L., et al., 2004. Nalp3 forms an Il-1beta-processing inflammasome with increased activity in Muckle-Wells autoinflammatory disorder. Immunity 20 (March 3), 319–325. https://doi.org/10.1016/s1074-7613(04)00046-9.

Akira, S., Uematsu, S., Takeuchi, O., 2006. Pathogen recognition and innate immunity. Cell 124 (February 4), 783–801. https://doi.org/10.1016/j.cell.2006.02.015.

Allen, I.C., et al., 2009. The Nlrp3 inflammasome mediates in vivo innate immunity to influenza a virus through recognition of viral rna. Immunity 30 (April 4), 556–565. https://doi.org/10.1016/j.immuni.2009.02.005.

Barnett, J.A., 2003. A history of research on yeasts 5: the fermentation pathway. Yeast 20 (April 6), 509–543. https://doi.org/10.1002/yea.986.

Brand, M.D., Nicholls, D.G., 2011. Assessing mitochondrial dysfunction in cells. Biochem. J 435 (April 2), 297–312. https://doi.org/10.1042/BJ20110162.

Chandler, J.D., et al., 2016. Metabolic pathways of lung inflammation revealed by High-Resolution metabolomics (hrm) of H1n1 influenza virus infection in mice. Am J Physiol Regul Integr Comp Physiol 311 (November 5), R906–R916. https://doi.org/10.1152/ajpregu.00298.2016.

Cline, T.D., Beck, D., Bianchini, E., 2017. Influenza virus replication in macrophages: balancing protection and pathogenesis. J. Gen. Virol. 98 (October10), 2401–2412. https://doi.org/10.1099/jgv.0.000922.

Crozat, K., Beutler, B., 2004. Tlr7: a New sensor of viral infection. Proc Natl Acad Sci U S A 101 (May 18), 6835–6836. https://doi.org/10.1073/pnas.0401347101.

Das, U.N., 2006. Pyruvate Is an endogenous anti-inflammatory and anti-oxidant molecule. Med Sci Monit 12 (May 5), RA79–84.

Diers, A.R., et al., 2012. Pyruvate fuels mitochondrial respiration and proliferation of breast cancer cells: effect of monocarboxylate transporter inhibition. Biochem. J 444 (June 3), 561–571. https://doi.org/10.1042/BJ20120294.

Halestrap, A.P., Price, N.T., 1999. The proton-linked monocarboxylate transporter (mct) family: structure, function and regulation. Biochem. J 343 (October Pt 2), 281–299.

Han, H., et al., 2020. Profiling serum cytokines in covid-19 patients reveals Il-6 and Il-10 are disease severity predictors. Emerg Microbes Infect 9 (December 1), 1123–1130. https://doi.org/10.1080/22221751.2020.1770129.

Heid, M.E., et al., 2013. Mitochondrial reactive oxygen species induces Nlrp3-dependent lysosomal damage and inflammasome activation. J. Immunol. 191 (November 10), 5230–5238. https://doi.org/10.4049/jimmunol.1301490.

Horby, Peter, et al., 2020. Effect of dexamethasone in hospitalized patients with covid-19: preliminary report. MedRxiv. https://doi.org/10.1101/2020.06.22.20137273. 2020-06-22.

Huo, C., et al., 2018. Lethal influenza a virus preferentially activates Tlr3 and triggers a severe inflammatory response. Virus Res 257 (09), 102–112. https://doi.org/10.1016/j.virusres.2018.09.012.

Karmen, A., Wroblewski, F., Ladue, J.S., 1955. Transaminase activity in human blood. J. Clin. Invest. 34 (January 1), 126–131. https://doi.org/10.1172/JCI103055.

Kato, H., et al., 2006. Differential roles of Mda5 and rig-I helicases in the recognition of rna viruses. Nature 441 (May 7089), 101–105. https://doi.org/10.1038/nature04734.

Kido, H., et al., 2016. Energy metabolic disorder Is a Major risk factor in severe influenza virus infection: proposals for New therapeutic options based on animal model experiments. Respir Investig 54 (September 5), 312–319. https://doi.org/10.1016/j.resinv.2016.02.007.

Lupfer, C., et al., 2008. Inhibition of influenza a H3n8 virus infections in mice by morpholino oligomers. Arch. Virol 153 (5), 929–937. https://doi.org/10.1007/s00705-008-0067-0.

Lupfer, C., et al., 2013. Receptor interacting protein kinase 2-mediated mitophagy regulates inflammasome activation during virus infection. Nat. Immunol. 14 (May 5), 480–488. https://doi.org/10.1038/ni.2563.

Lupfer, C.R., et al., 2014. Reactive oxygen species regulate caspase-11 expression and activation of the Non-canonical Nlrp3 inflammasome during enteric pathogen infection. PLoS Pathog. 10 (September 9), e1004410. https://doi.org/10.1371/journal.ppat.1004410.

Mariathasan, S., et al., 2006. Cryopyrin activates the inflammasome in response to toxins and atp. Nature 440 (March 7081), 228–232. https://doi.org/10.1038/nature04515.

Matarese, G., Procaccini, C., De Rosa, V., 2008. The intricate interface between immune and metabolic regulation: a role for leptin in the pathogenesis of multiple sclerosis? J. Leukoc. Biol. 84 (October 4), 893–899. https://doi.org/10.1189/jlb.0108022.

Moon, J.S., et al., 2015. Mtorc1-induced Hk1-dependent glycolysis regulates Nlrp3 inflammasome activation. Cell Rep 12 (July 1), 102–115. https://doi.org/10.1016/j.celrep.2015.05.046.

Morgan, M.J., Liu, Z.G., 2011. Crosstalk of reactive oxygen species and Nf-kappab signaling. Cell Res. 21 (January 1), 103–115. https://doi.org/10.1038/cr.2010.178.

Petrilli, V., et al., 2007. Activation of the Nalp3 inflammasome Is triggered by Low intracellular potassium concentration. Cell Death Differ. 14 (September 9), 1583–1589. https://doi.org/10.1038/sj.cdd.4402195.

Ramos-Ibeas, P., et al., 2017. Pyruvate antioxidant roles in human fibroblasts and embryonic stem cells. Mol. Cell. Biochem. 429 (May 1-2), 137–150. https://doi.org/10.1007/s11010-017-2942-z.

Roiniotis, J., et al., 2009. Hypoxia prolongs Monocyte/Macrophage survival and enhanced glycolysis Is associated with their maturation under aerobic conditions. J. Immunol. 182 (June 12), 7974–7981. https://doi.org/10.4049/jimmunol.0804216.

Schell, J.C., Rutter, J., 2013. The Long and Winding Road to the mitochondrial pyruvate carrier. Cancer Metab 1 (January 1), 6. https://doi.org/10.1186/2049-3002-1-6.

Selvaraj, V., et al., 2020. Short-term dexamethasone in sars-cov-2 patients. R I Med J (2013) 103 (June 6), 39–43.

Seth, R.B., et al., 2005. Identification and characterization of mavs, a mitochondrial antiviral signaling protein that activates Nf-Kappab and Irf 3. Cell 122 (September 5), 669–682. https://doi.org/10.1016/j.cell.2005.08.012.

Shi, L.Z., et al., 2011. Hif1alpha-dependent glycolytic pathway orchestrates a metabolic checkpoint for the differentiation of Th17 and treg cells. J. Exp. Med. 208 (July 7), 1367–1376. https://doi.org/10.1084/jem.20110278.

Smallwood, H.S., et al., 2017. Targeting metabolic reprogramming by influenza infection for therapeutic intervention. Cell Rep 19 (May 8), 1640–1653. https://doi.org/10.1016/j.celrep.2017.04.039.

Sutterwala, F.S., et al., 2006. Critical role for Nalp3/Cias1/Cryopyrin in innate and adaptive immunity through its regulation of caspase-1. Immunity 24 (March 3), 317–327. https://doi.org/10.1016/j.immuni.2006.02.004.

Theoharides, T.C., Conti, P., 2020. Dexamethasone for covid-19? Not so fast. J. Biol. Regul. Homeost. Agents 34 (June 3). https://doi.org/10.23812/20-EDITORIAL_1-5.

Trompette, A., et al., 2018. Dietary fiber confers protection against flu by shaping Ly6c(-) patrolling monocyte hematopoiesis and Cd8(+) T cell metabolism. Immunity 48 (May 5), 992–1005. https://doi.org/10.1016/j.immuni.2018.04.022.

Vander Heiden, M.G., Cantley, L.C., Thompson, C.B., 2009. Understanding the Warburg effect: the metabolic requirements of cell proliferation. Science 324 (May 5930), 1029–1033. https://doi.org/10.1126/science.1160809.

Votto, J.J., et al., 2008. Inhaled sodium pyruvate improved Fev1 and decreased expired breath levels of nitric oxide in patients with chronic obstructive pulmonary disease. J Aerosol Med Pulm Drug Deliv 21 (December 4), 329–334. https://doi.org/10.1089/jamp.2007.0678.

Xia, S., et al., 2016. Addition of sodium pyruvate to stored Red blood cells attenuates liver injury in a murine transfusion model. Mediators Inflamm. 2016, 3549207. https://doi.org/10.1155/2016/3549207.

Xie, M., et al., 2016. Pkm2-dependent glycolysis promotes Nlrp3 and Aim2 inflammasome activation. Nat. Commun. 7 (October), 13280. https://doi.org/10.1038/ncomms13280.

Zhang, W., et al., 2019. Lactate Is a natural suppressor of rlr signaling by targeting mavs. Cell 178 (June 1), 176–189. https://doi.org/10.1016/j.cell.2019.05.003. e15.